Determining effects of doping lithium nickel oxide with tungsten using Compton scattering

Veenavee Nipunika Kothalawala ✉ ⓘ ; Kosuke Suzuki ⓘ ; Xin Li ⓘ ; Bernardo Barbiellini ⓘ ; Johannes Nokelainen ⓘ ; Ilja Makkonen ⓘ ; Rafael Ferragut ⓘ ; Pekka Tynjälä ⓘ ; Petteri Laine ⓘ ; Juho Välikangas ⓘ ; Tao Hu ⓘ ; Ulla Lassi ⓘ ; Kodai Takano; Naruki Tsuji ⓘ ; Yosuke Amada; Assa Aravindh Sasikala Devi ⓘ ; Matti Alatalo ⓘ ; Yoshiharu Sakurai ⓘ ; Hiroshi Sakurai ⓘ ; Mohammad Babar; Venkatasubramanian Vishwanathan; Hasnain Hafiz; Arun Bansil ⓘ

Check for updates

View Online   Export Citation

AIP Publishing

Determining effects of doping lithium nickel oxide with tungsten using Compton scattering

View Online   Export Citation   CrossMark

Veenavee Nipunika Kothalawala,[1,a)] 🆔 Kosuke Suzuki,[2] 🆔 Xin Li,[1,3] 🆔 Bernardo Barbiellini,[1,4] 🆔
Johannes Nokelainen,[1,4] 🆔 Ilja Makkonen,[5] 🆔 Rafael Ferragut,[3] 🆔 Pekka Tynjälä,[6,7] 🆔 Petteri Laine,[6,7] 🆔
Juho Välikangas,[6,7] 🆔 Tao Hu,[6] 🆔 Ulla Lassi,[6,7] 🆔 Kodai Takano,[2] Naruki Tsuji,[8] 🆔 Yosuke Amada,[2]
Assa Aravindh Sasikala Devi,[6,9] 🆔 Matti Alatalo,[10] 🆔 Yoshiharu Sakurai,[8] 🆔 Hiroshi Sakurai,[2] 🆔
Mohammad Babar,[11] Venkatasubramanian Vishwanathan,[11] Hasnain Hafiz,[4] and Arun Bansil[4] 🆔

AFFILIATIONS

[1] Department of Physics, School of Engineering Science, LUT University, FI-53851 Lappeenranta, Finland
[2] Graduate School of Science and Technology, Gunma University, Kiryu, Gunma 376-8515, Japan
[3] L-NESS and Department of Physics, Politecnico di Milano, Via Anzani 42, 22100 Como, Italy
[4] Department of Physics, Northeastern University, Boston, Massachusetts 02115, USA
[5] Department of Physics, University of Helsinki, P.O. Box 43, FI-00014, University of Helsinki, Helsinki, Finland
[6] Research Unit of Sustainable Chemistry, University of Oulu, Oulu, Finland
[7] Kokkola University Consortium Chydenius, University of Jyvaskyla, Kokkola, Finland
[8] Japan Synchrotron Radiation Research Institute (JASRI), Sayo, Hyogo 679-5198, Japan
[9] Materials and Mechanical Engineering Research Unit, University of Oulu, Oulu, Finland
[10] Nano and Molecular Systems Research Unit, University of Oulu, Pentti Kaiteran Katu 1, 90570 Oulu, Finland
[11] Department of Aerospace Engineering, University of Michigan, Ann Arbor, Michigan 48109, USA

[a)] Author to whom correspondence should be addressed: veenavee.kothalawala@lut.fi

ABSTRACT

X-ray Compton scattering experiments along with parallel first-principles computations were carried out on $LiNiO_2$ to understand the effects of W doping on this cathode material for Li-ion batteries. By employing high-energy x rays exceeding 100 keV, an insight is gained into the fate of the W valence electrons, which are adduced to undergo transfer to empty O $2p$ energy bands within the active oxide matrix of the cathode. The substitution of W for Ni is shown to increase the electronic conductivity and to enhance the total magnetization per Ni atom. Our study demonstrates that an analysis of line shapes of Compton scattered x rays in combination with theoretical modeling can provide a precise method for an atomic level understanding of the nature of the doping process.

I. INTRODUCTION

With a rich history spanning over a century, nickel (Ni)-based cathodes have evolved from early alkaline rechargeable batteries to the prominent Ni-rich variant in lithium-ion batteries (LIBs).[1] Despite the initial dominance of $LiCoO_2$ in LIBs, Ni-based cathodes have come back in the mainstream battery industry due to their unique ability to provide high energy density and storage capacity at low cost.[2,3] The physical and chemical properties of $LiNiO_2$ (LNO) play a crucial role in driving the underlying redox reactions responsible for the superior performance of LNO as a battery material despite the challenges of structural and thermal stability.[4] Improvements for large scale applications have been realized by applying surface coating techniques and adjustments to the composition via atomic substitutions, which promise an enhanced battery performance.[5]

28 September 2024 17:53:36

Recent investigations[6–13] have focused on the effects of tungsten (W) doping on nickel-rich lithium-ion battery cathodes in LNO (WLNO) for improved energy density and overall battery performance. W doping acts to stabilize the crystal structure of the cathode, mitigate phase transitions, and improve longevity during charge/discharge cycles. W also enhances the electronic conductivity and thus facilitates electron transport and actively participates in oxygen redox reactions in nickel-rich cathodes to improve battery safety and stability.

Here, we employ high-energy x-ray Compton scattering experiments in combination with first-principles modeling to unravel fundamental quantum mechanical aspects of W doping on LNO. Through an analysis of the line shape of the Compton-scattered x rays, we adduce an atomic level understanding of how W influences the electronic structure of the LNO cathode. Our study contributes to the understanding of doping effects in LIBs for advancing battery performance and efficiency.

II. METHODS

A. Compton profiles

The Compton scattering profile is determined by the electron momentum density distribution, and within the *impulse approximation*,[14] it is given by the double differential cross section,

$$\frac{\mathrm{d}^2\sigma}{\mathrm{d}\Omega\mathrm{d}E} = F \cdot J(p_z), \tag{1}$$

where an explicit form for F was obtained by Eisenberger and Platzman.[15] The double differential cross section is thus proportional to the Compton profile $J(p_z)$, which is related to the ground-state electron momentum density $\rho(\mathbf{p})$,

$$J(p_z) = \iint \rho(\mathbf{p})\, \mathrm{d}p_x\, \mathrm{d}p_y, \tag{2}$$

where $\mathbf{p} = (p_x, p_y, p_z)$ is the electron momentum and p_z is taken to lie along the direction of the scattering vector. The momentum density of the occupied states under the independent particle approximation can be expressed as[16]

$$\rho(\mathbf{p}) = \sum_j \left| \int \psi_j(\mathbf{r}) e^{-i\mathbf{p}\mathbf{r}} d^3\mathbf{r} \right|^2, \tag{3}$$

where $\psi_j(\mathbf{r})$ are the Bloch wave functions or Kohn–Sham orbitals[17,18] that also give the valence contribution of the Compton profile line shape.[19–21] The core contribution can be obtained from the tabulated Hartree–Fock data.[22] See Ref. 23 for the details of the methodology.

To calculate the electronic structure and the Bloch wave functions of WLNO and LNO, we employed density functional theory (DFT) as implemented in the Vienna *Ab initio* Simulation Package (VASP),[24,25] based on projector-augmented waves.[26] The Perdew, Burke, and Ernzerhof (PBE) version of the generalized gradient approximation (GGA) was employed to treat exchange–correlation effects.[27] A plane wave basis set with a kinetic energy cutoff of 470 eV was used. To account for strong electron correlation effects, a Hubbard parameter $U = 4$ eV was applied to Ni 3d electrons, consistent with prior studies.[28,29]
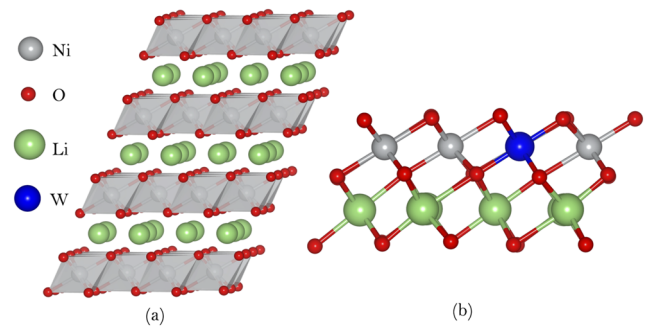

FIG. 1. (a) Layered LNO structure and (b) relaxed WLNO supercell for the 12.5% case. VESTA has been used for plotting.[31]

We simulated W dopings of 12.5%, 3%, and 1% using $2 \times 2 \times 1$, $2 \times 4 \times 2$, and $4 \times 4 \times 3$ supercells, respectively. For the pristine LNO, we employed the monoclinic crystal structure with an 8-atom primitive cell, characterized by a = 4.84/Å, b = 2.81/Å, and c = 5.12/Å (description here, how many atoms, lattice constants, crystal structure). The 12.5% case is illustrated in Fig. 1. The k-space grids used in the relaxation and Compton profiles calculations had a density of at least 0.02 2π/Å. The density of states (DOS) was computed with the tetrahedron method and with finer k meshes: for 12.5% and 3% cases as well as for LNO, we used $8 \times 8 \times 8$, and for 1% case, we used $3 \times 5 \times 4$ grids. VASPKIT was employed for postprocessing the VASP results.[30]

B. Synthesis of WLNO

Samples were synthesized using the method described by Välikangas *et al.*,[3,5] which involved the following steps. *Coprecipitation of* $Ni(OH)_2$: Spherical $Ni(OH)_2$ precursor was first synthesized using alkali metal hydroxide (NaOH) coprecipitation in an inert gas (nitrogen) atmosphere.[32] An inert gas was used to prevent the oxidation of the precursor. Precipitation was done in a continuous-flow stirred-tank reactor (CSTR) with a reactor volume of 3 l at 50 °C under vigorous agitation. Particle size growth during coprecipitation was followed by determining the particle size distribution of the slurry sampled from the reactor's overflow tubing. The solution was heated to a precipitation temperature, and the pH was adjusted to the desired level with a NaOH solution. The feeding rates of nickel sulfate, Na_2WO_3, NaOH, and ammonia solutions were adjusted to maintain the desired residence time. After coprecipitation, the precursor slurry was filtered in a vacuum, and the precipitate was carefully washed with a sufficient amount of warm deionized water. The synthesized 1 mol. % W–$Ni(OH)_2$ precursors were dried overnight at 60 °C in a vacuum oven. *Lithiation*: The 1 mol. % W–$Ni(OH)_2$ precursor was mixed with LiOH using a Li:Ni:W molar ratio of 1:1. This was followed by calcination at 690 °C. Excess LiOH was used to compensate for lithium loss during high-temperature calcination and to ensure homogeneous lithiation. The mixture was calcined with a 2.5 °C min^{-1} heating ramp and a 5 h holding time at 690 °C in an oxygen atmosphere and subsequently milled and sieved to less than 40 μm under dry room conditions; see Välikangas *et al.*[3] for details. Inductively Coupled Plasma (ICP) spectroscopy measurements of the WLNO samples found an excess

of lithium with a Li/Ni ratio of about 1.02, but we estimate that this ratio could be as large as 1.03 since excess of Li was used in our synthesis process.

C. Experimental Compton profiles

The spherically averaged WLNO Compton profiles were measured at the high-energy inelastic x-ray scattering beamline BL08W at the Japanese synchrotron facility SPring-8[33,34] with the same experimental setup as in our previous LNO study[35] to maintain consistency in analyzing the results. Circularly polarized x rays with an energy of 182.6 keV, emitted from an elliptical multipole wiggler, were directed onto the sample. The incident x-ray beam at the sample position had a cross-sectional area of 1 mm^2. The Compton scattered x rays were detected using a pure Ge solid-state detector. The scattering angle was fixed at 178°, and the Compton profiles were measured at room temperature. The overall momentum resolution of the equipment was 0.5 a.u., sufficient to reveal the details of valence orbitals in cathode materials.[35] To suppress Compton scattering by air, the sample was arranged in a vacuum chamber and the measurements were performed under vacuum conditions. The sample structure was verified by XRD (Rigaku SmartLab) measurements using CuKa radiation. The diffraction patterns of the sample display a high integrated intensity ratio of I(003)/I(104), which confirms the layered character of the crystal structure.[3]
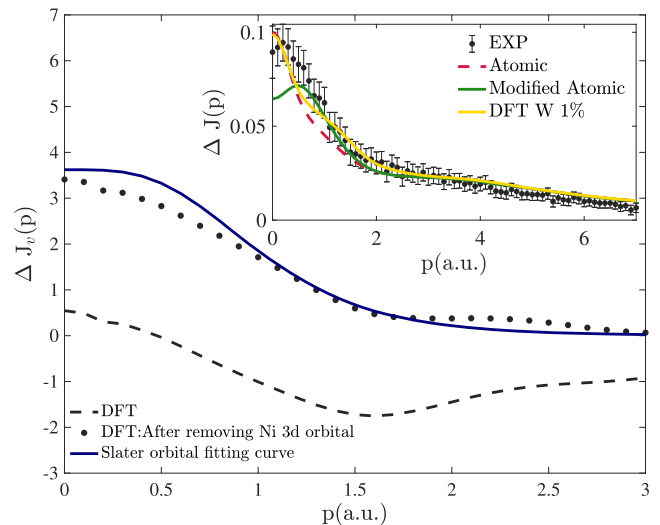
III. RESULTS AND DISCUSSION

The experimental Compton profiles are shown in Fig. 2. The explanation of the normalization of these curves is as follows: Ideally, the pristine LNO profile is normalized to 47 electrons (core plus valence) across the entire momentum range. However, in our case, the momentum range is limited to a 10 a.u. cutoff. Therefore, the
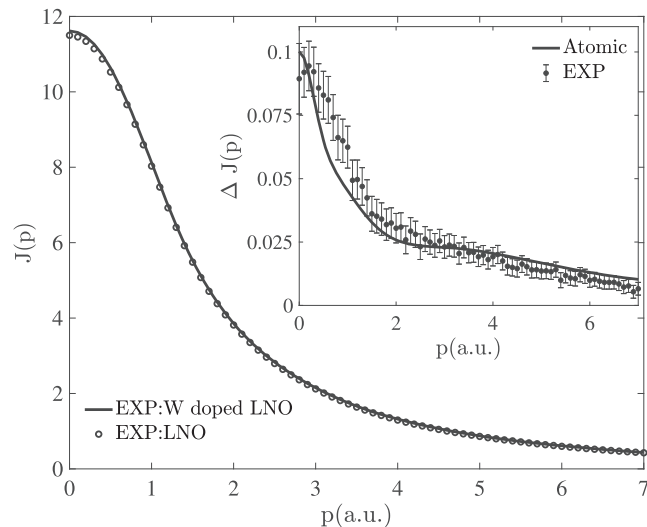
normalization should be smaller than 47. This number can be estimated using the Biggs' atomic profiles since these profiles become exact at high momenta. For WLNO, the normalization on the complete momentum range yielded 47.55 electrons, corresponding to 1% W concentration ($Z = 74$) replacing Ni ($Z = 28$) and an excess of Li, resulting in a Li/Ni ratio of 1.03, optimizing the shape of the Compton profile tail. In addition, for pristine LNO, the total number of electrons is slightly lower than 47 due to a small deficit of Li atoms, detected via ICP (see the supplementary material of Ref. 35), now estimated at 2% through fitting with the Compton profile tails. The inset of Fig. 2 shows $\Delta J(p)$ defined as the difference between the Compton profiles of the WLNO doped material and the Compton profile of the pristine LNO material. The profile difference $\Delta J(p)$ facilitates the interpretation of electronic structure changes induced by W doping because many irrelevant contributions are thus subtracted out. Interestingly, the amplitude of $\Delta J(p)$ can be explained with a simple model of the Compton profile based on Hartree–Fock atomic orbitals;[22] see also Suzuki et al.[36] for a discussion of Compton profile changes due to lithiation in cathode materials.

Patel et al.[37] observed that the atomic model used to describe the Compton profile of LIBs can be refined by substituting the Li 2s valence electron with an electron in the O 2p orbital. This replacement reflects the transfer of one electron from the Li atom to a neighboring oxygen atom, resulting in Li atoms becoming a cation Li$^+$. Here, we investigate whether a similar transfer occurs for the six

FIG. 2. Spherically averaged total experimental Compton profiles. The inset shows the total Compton profile difference between the experimental and atomic WLNO (W-doped LNO) and pristine LNO. The experiment shows the error bars. The curve labeled "atomic" in the inset (solid line) refers to the Compton profiles based on Hartree–Fock atomic orbitals.

FIG. 3. Spherically averaged valence Compton profile differences, $\Delta J_v(p)$, between WLNO and LNO (WLNO – LNO) calculated with DFT for a W concentration of 12.5% (black dashed line). The black dotted line corresponds to the case where the eight 3d electrons of Ni are removed by treating them as core electrons; this curve can be fitted with the profile of a Slater O (2p) orbital (blue solid line). The inset shows the total Compton profile differences as in the inset of Fig. 2; the curve labeled "atomic" (red dashed line) refers to the computed profiles based on Hartree–Fock atomic orbitals, while the curve labeled "modified atomic" (green solid line) refers to an improved model in which the contributions from excess Li atoms and W atoms are replaced by those for the Slater O (2p) orbital given in the main figure. Finally, the curve labeled "DFT W 1%" (yellow solid line) incorporates the results of the DFT calculation at 1% W concentration for the W–Ni valence contribution.

valence electrons of W dopants in WLNO, leading to the formation of W^{6+} ion[12] with W valence electrons moving into the O $2p$ orbital. Recently, it has been shown[4] that the ionic charges in LNO can be rationalized as Ni^{2+}, $O^{1.5-}$, and Li^+. If the W impurity goes into a Ni site, then a W^{6+} ion replaces a Ni^{2+} ion, and the four extra valence electrons occupy the O $2p$ states. In our VASP calculation, Ni has 10 valence electrons, but eight Ni $3d$ electrons are more localized and less active.[4] Therefore, the contribution of these eight atomic-like $3d$ electrons of Ni can be approximately removed from the Compton valence profile of Ni by using their Compton profile based on atomic orbitals.[22]

To analyze the valence Compton profile differences $\Delta J_v(p)$ between WLNO and LNO, we consider the case with a W concentration of 12.5% since a simple picture emerges. In the main panel of Fig. 3, we consider the profile in which the contributions of Ni $3d$ states are excluded by treating them as core states. In this case, one can easily justify that the four extra valence electrons are transferred to the O $2p$ states since the curve can be fitted by the profile of an O $2p$ Slater orbital used previously by Kothalawala *et al.*[35] In this connection, we note that the sample is fully metallic at 12.5% W doping and the LNO energy gap vanishes already with 3% W doping as shown Fig. 4. Our results are consistent with the finding of Gao *et al.*[12] that W doping improves the conductivity of LNO. Finally, the inset of Fig. 3 shows that the agreement between theory and experiment $\Delta J(p)$ shows an overall improvement if the contribution of the Li excess and W is replaced by the Slater O $2p$ orbital. As expected, the resulting "modified atomic model" (green solid line in the inset) rationalizes the strong O $2p$ weight in the partial DOS (PDOS),
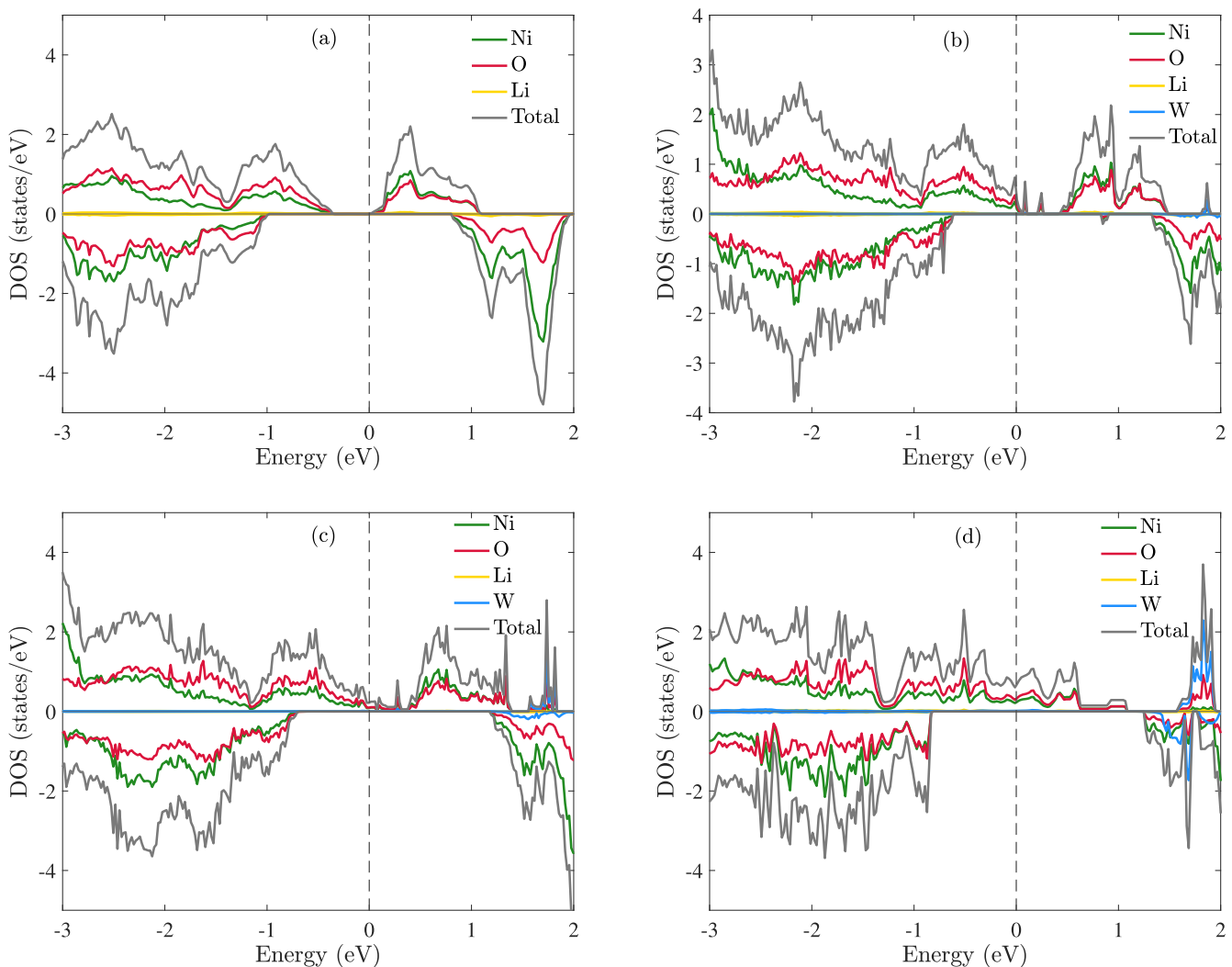
FIG. 4. Closing of the spin majority states' energy gap with W doping. Total and partial density of states in (a) pristine LNO, (b) WLNO with 1% W doping, (c) WLNO with 3% W doping, and (d) WLNO with 12.5% W doping. The upper and lower portions of all figures give up-spin (majority spin) and down-spin (minority spin) contributions to the densities of states. The DOS are normalized to the formula units.
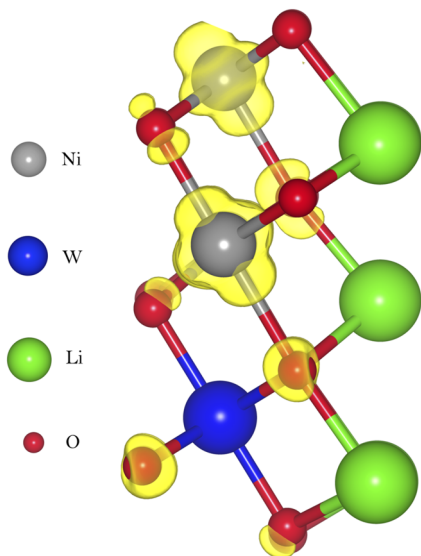
FIG. 5. Magnetization density in 12.5% W doped LNO using an isosurface value of 0.01 a.u.

Fig. 4(b) (red line); a significant Ni weight in the PDOS is also visible due to a strong nickel–oxygen hybridization.[35] If we incorporate the results of the DFT calculation at 1% W concentration for the W–Ni contribution instead of using the simple Slater O $2p$ orbital contribution used in the modified atomic model, we observe an impressive agreement with experiment also at low momenta.

Another DFT calculation[38] involving W doping, which considers charge density changes in LNO, shows that the introduction of W increases the charge density around O atoms more than around Ni atoms. Our simulations reflect this trend since our Bader analysis results show that the oxygen ions acquire on average 1.2 electrons around Ni and 1.7 electrons around W sites. We thus infer that the charge density around the O atoms plays an important role in enhancing electron conductivity in WLNO by generating an increase in the number of itinerant electrons.

Our calculations confirm the ferromagnetic phase of LNO [Fig. 4(a)], which was reported by Goodenough *et al.* as far back as 1958.[39] W doping increases the average magnetic moment per Ni atom. Interestingly, the magnetization density distribution in WLNO (Fig. 5) shows the appearance of significant magnetization on the oxygen ions neighboring W impurities. In our calculations, we determined that the total magnetic moment per Ni ion in LNO amounts to 1 μ_B.[29,35] Upon introducing a 1% concentration of W into the sample, this average magnetic moment increases to 1.02 μ_B. With a 3% concentration of W, the average magnetic moment further rises to 1.08 μ_B per Ni ion. Interestingly, at a concentration of 12.5%, the magnetic moment reaches 1.29 μ_B per Ni ion. Moreover, Fig. 5 shows that the magnetic moment mostly changes on the oxygen sites, while remains similar on the Ni ions.

IV. CONCLUSIONS

Our first-principles calculations, coupled with Compton scattering experiments, show that the substitution of W by Ni in LNO enhances the electronic conductivity and the ferromagnetic phase. Hafiz *et al.*[40] have pointed to the role of itinerant ferromagnetic phases for obtaining an improved battery performance. Our analysis reveals that W valence electrons in WLNO undergo transfer to the O $2p$ itinerant states and gives an insight into the chemistry of W incorporation on LNO. Our study shows how, by combining x-ray Compton scattering measurements with parallel first-principles modeling, an atomic level understanding of doping effects can be obtained toward the rational design of battery materials.

AUTHOR DECLARATIONS

Conflict of Interest

The authors have no conflicts to disclose.

Author Contributions

Veenavee Nipunika Kothalawala: Conceptualization (equal); Formal analysis (lead); Investigation (equal); Methodology (equal); Visualization (lead); Writing – original draft (equal). **Kosuke Suzuki**: Data curation (equal); Formal analysis (equal); Methodology (equal); Validation (equal); Writing – review & editing (equal). **Xin Li**: Methodology (supporting); Writing – review & editing (supporting). **Bernardo Barbiellini**: Conceptualization (equal); Formal analysis (equal); Investigation (equal); Methodology (equal); Supervision (lead); Writing – original draft (equal); Writing – review & editing (lead). **Johannes Nokelainen**: Data curation (equal); Investigation (equal); Methodology (equal); Supervision (equal); Visualization (equal); Writing – original draft (equal); Writing – review & editing (supporting). **Ilja Makkonen**: Conceptualization (equal); Formal analysis (equal); Methodology (lead); Supervision (equal); Validation (equal); Writing – review & editing (lead). **Rafael Ferragut**: Writing – review & editing (equal). **Pekka Tynjälä**: Conceptualization (equal); Investigation (equal); Methodology (equal); Validation (equal). **Petteri Laine**: Conceptualization

(equal); Investigation (equal); Methodology (equal); Validation (equal). **Juho Välikangas**: Conceptualization (equal); Investigation (equal); Methodology (equal); Validation (equal). **Tao Hu**: Conceptualization (equal); Investigation (equal); Methodology (equal); Validation (equal). **Ulla Lassi**: Conceptualization (equal); Investigation (equal); Methodology (equal); Supervision (equal); Writing – review & editing (equal) **Kodai Takano**: Methodology (supporting); Resources (equal); Validation (equal). **Naruki Tsuji**: Methodology (supporting); Resources (equal); Validation (equal). **Yosuke Amada**: Data curation (equal); Methodology (equal); Resources (equal). **Assa Aravindh Sasikala Devi**: Investigation (equal); Writing – review & editing (equal). **Matti Alatalo**: Investigation (equal); Writing – review & editing (equal). **Yoshiharu Sakurai**: Methodology (equal); Resources (equal); Writing – review & editing (equal). **Hiroshi Sakurai**: Conceptualization (equal); Formal analysis (equal); Investigation (equal); Methodology (equal); Writing – review & editing (equal). **Mohammad Babar**: Writing – review & editing (supporting). **Venkat Vishwanathan**: Writing – review & editing (supporting). **Hasnain Hafiz**: Writing – review & editing (supporting). **Arun Bansil**: Investigation (equal); Methodology (equal); Writing – review & editing (lead).

DATA AVAILABILITY

The data that support the findings of this study are openly available in the GitHub repository at https://github.com/Veenavi92/W-doped-LiNiO2.

REFERENCES

[1]L. Wang, J. Wang, L. Wang, M. Zhang, R. Wang, and C. Zhan, "A critical review on nickel-based cathodes in rechargeable batteries," Int. J. Miner., Metall. Mater. **29**, 925–941 (2022).

[2]M. Bianchini, M. Roca-Ayats, P. Hartmann, T. Brezesinski, and J. Janek, "There and back again—The journey of LiNiO2 as a cathode active material," Angew. Chem., Int. Ed. **58**, 10434–10458 (2019).

[3]J. Välikangas, P. Laine, M. Hietaniemi, T. Hu, P. Tynjälä, and U. Lassi, "Precipitation and calcination of high-capacity LiNiO2 cathode material for lithium-ion batteries," Appl. Sci. **10**, 8988 (2020).

[4]A. R. Genreith-Schriever, H. Banerjee, A. S. Menon, E. N. Bassey, L. F. Piper, C. P. Grey, and A. J. Morris, "Oxygen hole formation controls stability in LiNiO2 cathodes," Joule **7**, 1623–1640 (2023).

[5]J. Välikangas, P. Laine, M. Hietaniemi, M. Selent, P. Tynjälä, and U. Lassi, "Correlation of aluminum doping and lithiation temperature with electrochemical performance of LiNiO2 cathode material," J. Solid State Electrochem. **27**, 641 (2022).

[6]H. H. Ryu, G. T. Park, C. S. Yoon, and Y.-K. Sun, "Suppressing detrimental phase transitions via tungsten doping of LiNiO2 cathode for next-generation lithium-ion batteries," J. Mater. Chem. A **7**, 18580–18588 (2019).

[7]S. Yoshio, K. Hongo, K. Nakano, and R. Maezono, "High-throughput evaluation of discharge profiles of nickel substitution in LiNiO2 by *ab initio* calculations," J. Phys. Chem. C **125**, 14517–14524 (2021).

[8]Y. Yoshimoto, T. Toma, K. Hongo, K. Nakano, and R. Maezono, "Computational design to suppress thermal runaway of Li-ion batteries via atomic substitutions to cathode materials," ACS Appl. Mater. Interfaces **14**, 23355–23363 (2022).

[9]C. Geng, D. Rathore, D. Heino, N. Zhang, I. Hamam, N. Zaker, G. A. Botton, R. Omessi, N. Phattharasupakun, T. Bond, C. Yang, and J. R. Dahn, "Mechanism of action of the tungsten dopant in LiNiO2 positive electrode materials," Adv. Energy Mater. **12**, 2103067 (2022).

[10]Y. Liu, X. Wen, R. K. Lake, and J. Guo, "First-principles study of the doping effect in half delithiated LiNiO2 cathodes," ACS Appl. Energy Mater. **6**, 2134–2139 (2023).

[11]N. Zaker, C. Geng, D. Rathore, I. Hamam, N. Chen, P. Xiao, C. Yang, J. R. Dahn, and G. A. Botton, "Probing the mysterious behavior of tungsten as a dopant inside pristine cobalt-free nickel-rich cathode materials," Adv. Funct. Mater. **33**, 2211178 (2023).

[12]D. Gao, W. Che, Q. Xu, X. Zhao, Y. Huang, and C. Chang, "W doping improves the electrochemical performance of $Li_xNi_{0.94}Co_{0.04}Al_{0.02}O_2$ cathode through dual enhanced electronic and ionic conductivities: A study from DFT calculations and experimental results," Scr. Mater. **234**, 115586 (2023).

[13]A. Menon, B. Johnston, S. Booth, L. Zhang, K. Kress, B. Murdock, G. Paez Fajardo, N. Anthonisamy, N. Tapia-Ruiz, S. Agrestini, M. Garcia-Fernandez, K. Zhou, P. Thakur, T. Lee, A. Nedoma, S. Cussen, and L. Piper, "Oxygen-redox activity in non-lithium-excess tungsten-doped LiNiO2 cathode," PRX Energy **2**, 013005 (2023).

[14]I. G. Kaplan, B. Barbiellini, and A. Bansil, "Compton scattering beyond the impulse approximation," Phys. Rev. B **68**, 235104 (2003).

[15]P. Eisenberger and P. M. Platzman, "Compton scattering of x rays from bound electrons," Phys. Rev. A **2**, 415–423 (1970).

[16]J. Nokelainen, B. Barbiellini, J. Kuriplach, S. Eijt, R. Ferragut, X. Li, V. Kothalawala, K. Suzuki, H. Sakurai, H. Hafiz *et al.*, "Identifying redox orbitals and defects in lithium-ion cathodes with Compton scattering and positron annihilation spectroscopies: A review," Condens. Matter **7**, 47 (2022).

[17]B. Barbiellini, "A natural orbital method for the electron momentum distribution in matter," J. Phys. Chem. Solids **61**, 341–344 (2000).

[18]B. Barbiellini and A. Bansil, "Treatment of correlation effects in electron momentum density: Density functional theory and beyond," J. Phys. Chem. Solids **62**, 2181–2189 (2001).

[19]D. Ernsting, D. Billington, T. Haynes, T. Millichamp, J. Taylor, J. Duffy, S. Giblin, J. Dewhurst, and S. Dugdale, "Calculating electron momentum densities and Compton profiles using the linear tetrahedron method," J. Phys.: Condens. Matter **26**, 495501 (2014).

[20]C. Gatti and P. Macchi, "A guided tour through modern charge density analysis," in *Modern Charge-Density Analysis* (Springer, 2011), pp. 1–78.

[21]A. Koizumi, S. Miyaki, Y. Kakutani, H. Koizumi, N. Hiraoka, K. Makoshi, N. Sakai, K. Hirota, and Y. Murakami, "Study of the e_g orbitals in the bilayer manganite $La_{2−2x}Sr_{1+2x}Mn_2O_7$ by using magnetic Compton-profile measurement," Phys. Rev. Lett. **86**, 5589 (2001).

[22]F. Biggs, L. Mendelsohn, and J. Mann, "Hartree-Fock Compton profiles for the elements," At. Data Nucl. Data Tables **16**, 201–309 (1975).

[23]I. Makkonen, M. Hakala, and M. Puska, "Calculation of valence electron momentum densities using the projector augmented-wave method," J. Phys. Chem. Solids **66**, 1128–1135 (2005).

[24]G. Kresse and J. Furthmüller, "Efficiency of *ab initio* total energy calculations for metals and semiconductors using a plane-wave basis set," Comput. Mater. Sci. **6**, 15 (1996).

[25]G. Kresse and D. Joubert, "From ultrasoft pseudopotentials to the projector augmented-wave method," Phys. Rev. B **59**, 1758–1775 (1999).

[26]P. E. Blöchl, "Projector augmented-wave method," Phys. Rev. B **50**, 17953–17979 (1994).

[27]J. Perdew, K. Burke, and M. Ernzerhof, "Generalized gradient approximation made simple," Phys. Rev. Lett. **77**, 3865–3868 (1996).

[28]M. Tuccillo, O. Palumbo, M. Pavone, A. Muñoz-García, A. Paolone, and S. Brutti, "Analysis of the phase stability of LiMO2 layered oxides (M = Co, Mn, Ni)," Crystals **10**, 526 (2020).

[29]V. N. Kothalawala, A. A. Sasikala Devi, J. Nokelainen, M. Alatalo, B. Barbiellini, T. Hu, U. Lassi, K. Suzuki, H. Sakurai, and A. Bansil, "First principles calculations of the optical response of LiNiO2," Condens. Matter **7**, 54 (2022).

[30]V. Wang, N. Xu, J.-C. Liu, G. Tang, and W.-T. Geng, "VASPKIT: A user-friendly interface facilitating high-throughput computing and analysis using VASP code," Comput. Phys. Commun. **267**, 108033 (2021).

28 September 2024 17:53:36

[31] K. Momma and F. Izumi, "VESTA3 for three-dimensional visualization of crystal, volumetric and morphology data," J. Appl. Crystallogr. **44**, 1272–1276 (2011).

[32] P. Tynjälä, P. Laine, J. Välikangas, T. Kauppinen, and U. Lassi, "Effect of reaction conditions on the coprecipitation of $Ni(OH)_2$ for lithium-ion batteries," Chem. Eng. Technol. **46**, 2279–2284 (2023).

[33] Y. Sakurai, "High-energy inelastic-scattering beamline for electron momentum density study," J. Synchrotron Radiat. **5**, 208–214 (1998).

[34] Y. Kakutani, Y. Kubo, A. Koizumi, N. Sakai, B. L Ahuja, and B. K Sharma, "Magnetic Compton profiles of Fcc-Ni, $Fcc-Fe_{50}Ni_{50}$ and Hcp-Co," J. Phys. Soc. Jpn. **72**, 599–606 (2003).

[35] V. N. Kothalawala, K. Suzuki, J. Nokelainen, A. Hyvönen, I. Makkonen, B. Barbiellini, H. Hafiz, P. Tynjälä, P. Laine, J. Välikangas, T. Hu, U. Lassi, K. Takano, N. Tsuji, Y. Amada, A. A. S. Devi, M. Alatalo, Y. Sakurai, H. Sakurai, and A. Bansil, "Compton scattering study of strong orbital delocalization in a $LiNiO_2$ cathode," Phys. Rev. B **109**, 035139 (2024).

[36] K. Suzuki, B. Barbiellini, Y. Orikasa, S. Kaprzyk, M. Itou, K. Yamamoto, Y. J. Wang, H. Hafiz, Y. Uchimoto, A. Bansil et al., "Non-destructive measurement of in-operando lithium concentration in batteries via x-ray Compton scattering," J. Appl. Phys. **119**, 025103 (2016).

[37] U. Patel, T. Guruswamy, A. Krzysko, H. Charalambous, L. Gades, K. Wiaderek, O. Quaranta, Y. Ren, A. Yakovenko, U. Ruett, and A. Miceli, "High-resolution Compton spectroscopy using x-ray microcalorimeters," Rev. Sci. Instrum. **93**, 113105 (2022).

[38] Y. Liu, X. Wan, G. Daichao, C. Chang, and J. Zheng, "Synergistic effects of W and Na Co-doping on the electrochemical performance of Mn based Li-rich cathode: W enhances the electronic conductivity to improve the cyclability and Na increases the Li mobility to promote the rate behavior," Available at SSRN 4486464.

[39] J. Goodenough, D. Wickham, and W. Croft, "Some ferrimagnetic properties of the system $Li_xNi_{1-x}O$," J. Appl. Phys. **29**, 382–383 (1958).

[40] H. Hafiz, K. Suzuki, B. Barbiellini, Y. Orikasa, S. Kaprzyk, N. Tsuji, K. Yamamoto, A. Terasaka, K. Hoshi, Y. Uchimoto, Y. Sakurai, H. Sakurai, and A. Bansil, "Identification of ferrimagnetic orbitals preventing spinel degradation by charge ordering in $Li_xMn_2O_4$," Phys. Rev. B **100**, 205104 (2019).

28 September 2024 17:53:36